Order and dynamics in the lamellar L_α and in the hexagonal H_{II} phase

Dioleoylphosphatidylethanolamine studied with angle-resolved fluorescence depolarization

Herman van Langen, Charles A. Schrama, Gijs van Ginkel, Gerard Ranke, and Yehudi K. Levine
Department of Molecular Biophysics, Buys Ballot Laboratory, University of Utrecht, 3508 TA Utrecht, The Netherlands

ABSTRACT Fluorescence depolarization techniques are used to determine the molecular order and reorientational dynamics of the probe molecule TMA-DPH embedded in the lamellar L_α and the hexagonal H_{II} phases of lipid/water mixtures. The thermotropically induced $L_\alpha \rightarrow H_{II}$ phase transition of the lipid DOPE is used to obtain macroscopically aligned samples in the hexagonal H_{II} phase at 45°C from samples prepared in the lamellar L_α phase at 7°C. The interpretation of angle-resolved fluorescence depolarization experiments on these phases, within the framework of the rotational diffusion model, yields the order parameters $\langle P_2 \rangle$ and $\langle P_4 \rangle$, and the diffusion constants for the reorientational motions. The reorientational motion rates of the TMA-DPH molecules in the hexagonal H_{II} phase are comparable with those in the lamellar L_α phase. Furthermore, the lateral diffusion of the probe molecule on the surface of the lipid/water cylinder in the hexagonal phase is found to be considerably slower than the reorientational motion.

INTRODUCTION

The biological membrane is a flexible and dynamic structure and undergoes many conformational changes to accommodate its various functions. The membrane lipids are thought to play a vital role in these processes. Lipid polymorphism, the ability of lipids to organize in different macroscopic structures, may well be involved in these structural changes. This concept of membrane structure is based on a large number of model studies in which the lipid phase behavior was investigated. It has been shown that at physiological temperatures, variations in the experimental conditions such as ion concentration (e.g. Ca^{2+}), pH, degree of hydration of the lipid headgroups, and insertion of proteins into the lipid matrix can markedly affect the membrane structure and lipid phase transitions (Reiss-Husson, 1967; Luzzati et al., 1968; Ranck et al., 1977; Cullis and de Kruijff, 1978; Cullis et al., 1980; van Venetië and Verkleij, 1981; Rilfors et al., 1984; de Kruijff et al., 1985*a* and *b*; Gruner, 1985; Crowe et al., 1988).

These effects can be rationalized in terms of the elegant molecular shape concept proposed by Israelachvili and Mitchell (1975), for reviews see refs. (Rilfors et al., 1984; de Kruijff et al., 1985a; Israelachvili et al., 1980). In this concept it is assumed that the overall form of the lipid molecules, which is influenced by a number of structural and thermodynamic factors, determines the structure of the hydrated lipid matrix. For example lipids with the overall shape of a cylinder pack most efficiently in a planar bilayer structure on dispersion in water. On the other hand, if the cross-section of the lipid headgroup is larger than the cross-section of the hydrocarbon chains, the molecule has the overall shape of an inverted cone. Such cones are most easily packed in a micellar structure in water. The third possibility, where the cross-section of the lipid headgroup is smaller than that of the hydrocarbon chains, gives rise to a conical shape. These lipids pack preferentially in the hexagonal H_{II} phase on dispersion in water.

The environmental conditions are also expected to influence the overall shape of the lipid molecules so that structural transitions between the different macroscopic phases can be induced by changes in hydration and temperature. Cylindrically shaped hydrated lipids which are organized in planar bilayers can form a hexagonal structure at elevated temperatures. The temperature increase appears to change the balance between the cross-sections of the headgroup and hydrocarbon regions. A larger cross-section for the hydrocarbon region resulting from temperature-induced gauche defects in the acyl chains of the lipid molecule is now expected. This leads to more cone-shaped lipid molecules, which will organize in the hexagonal phase.

The bilayer-to-nonbilayer phase transitions have been widely investigated; in particular the thermotropically induced phase transition from the lamellar phase (L_α) to the inverted hexagonal phase (H_{II}) in phosphatidylethanolamines has been the subject of many studies (Cullis and de Kruijff, 1978; Cullis et al., 1980; van Venetië and Verkleij, 1981; Caffrey, 1985; Tate and Gruner, 1987; Bentz et al., 1987). The L_α phase is a lipid bilayer, 40 Å in thickness and separated by a water layer of 18 Å (Ranck et al., 1977; Cullis and de Kruijff, 1978; de Kruijff et al.,

0006-3495/89/05/937/10 $2.00

1985*a*; Blaurock, 1982). The hexagonal H_{II} phase consists of lipid/water tubes 10^4–10^5 Å in length with diameter of ~70 Å and a central water core of 30 Å in diameter (Reiss-Husson, 1967; Gruner, 1985; Caffrey, 1985). On a microscopic scale the $L_\alpha \rightarrow H_{II}$ phase transition requires a considerable rearrangement of lipid molecules (Kirk et al., 1984). Calculations on the formation of a precursor in the transition, the inverted micellar intermediate (IMI), have recently been presented (Siegel, 1986*a* and *b*). This precursor may be of biological interest for the description of processes related to membrane fusion and exocythosis.

A number of experimental techniques have been used to obtain structural information about the L_α and H_{II} phases. However none of these techniques provide a detailed picture of molecular order and reorientational dynamics of the lipid molecules in the hexagonal structure. X-Ray (Reiss-Husson, 1967; Luzzati et al., 1968; Gruner, 1985; Caffrey, 1985; Blaurock, 1982) and neutron diffraction techniques (Büldt et al., 1978) have been used to characterize the lattice constants, while differential scanning calorimetry (DSC) experiments have yielded phase transition temperatures and thermodynamic properties of the transition (Ellens et al., 1986; Brown et al., 1986; Gasset et al., 1988). On the other hand, nuclear magnetic resonance (NMR) (Cullis and de Kruijff, 1978; Cullis et al., 1980; de Kruijff et al., 1985*a*; Sjölund et al., 1987; Marsh and Seddon, 1982) and electron microscopy (van Venetië and Verkleij, 1981) have only been used to identify the phase of the samples. Electron spin resonance (ESR) spectra were also found to reflect the phase structure, but their detailed interpretation in terms of molecular behavior is not straightforward (Hardman, 1982; Lasic and Hauser, 1984). Finally we note that the phase transitions can also be monitored through the changes in the fluorescence intensity (Hong et al., 1988).

We have therefore undertaken a fluorescence depolarization study of the molecular order and reorientational dynamics of systems in the hexagonal phase using macroscopically ordered samples. The method has been previously applied by us to planar multibilayer systems (van Langen et al., 1987*a*; Deinum et al., 1988; Mulders et al., 1986) and detailed information about the molecular properties in these systems was obtained from the interpretation of angle-resolved fluorescence depolarization (AFD) experiments. Here we describe a modification of our previous work which is applicable to the study of hexagonal phases.

To justify the theoretical description of the experiment we have used the thermotropic $L_\alpha \rightarrow H_{II}$ phase transition of the lipid dioleoylphospatidylethanolamine (DOPE). It has been shown by NMR techniques that a sample oriented macroscopically between glass plates in the lamellar L_α phase retains the alignment in the hexagonal H_{II} phase (Cullis et al., 1980). In the L_α phase the bilayer planes are parallel to the glass plates, while in the H_{II} phase the lipid/water tubes possess this orientation (Mely et al., 1975). Nevertheless, the long axes of the tubes are uniformly distributed (uniaxial symmetry) around the normal to the glass plates. The fluorescent probe 1-[4-trimethyl ammonium phenyl]-6-phenyl-1,3,5-hexatriene (TMA-DPH) is used to monitor the behavior of the orientational order and the reorientational dynamics of the lipid molecules in the system.

THEORETICAL DESCRIPTION

Sample Geometry

In the hexagonal H_{II} phase the lipid molecules are ordered with their polar headgroups anchored at the long central water core of the cylinder, Fig. 1. On the other hand, the nonpolar lipid tails are directed away from this central water core. These lipid/water hexagons form a hexagonal lattice. On a microscopic scale these cylinders are organized in bundles while on a macroscopic scale the bundles are randomly oriented with their long axes parallel to the glass plates of the thin sample (Mely et al., 1975; Boggs and Hsia, 1973). The sample possesses a uniaxial symmetry about the normal to its surface.

The excitation light pulse, with polarization direction $\vec{e}_i$, is incident on the sample at an angle θ relative to the normal to the sample surface as depicted in Fig. 2. The director of the sample, the normal to its plane, defines the laboratory z-axis. The x- and y-axis are chosen so as to form a right-handed coordinate frame. The fluorescence light, polarized along the direction $\vec{e}_f$, is observed along an axis making an angle φ with the director, Fig. 2.

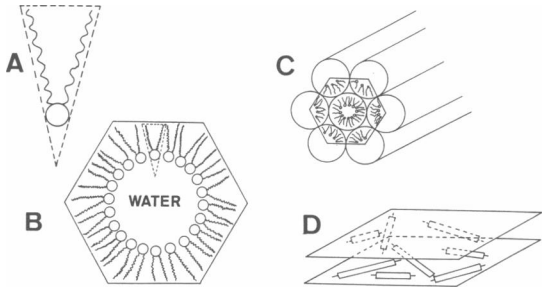

FIGURE 1 The sample structure of the hexagonal H_{II} phase. (*A*) a cone-shaped lipid molecule. (*B*) A molecular dispersion in water; tubes are formed having the cross-section of a hexagon. (*C*) in three dimensions these tubes are arranged in a hexagonal lattice forming bundles. (*D*) On macroscopic scale the long axes of these bundles are aligned parallel to the glass plates of the sample.

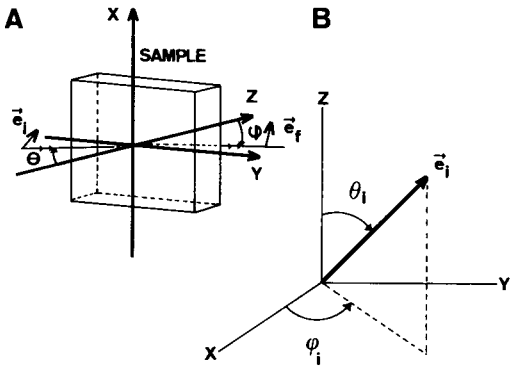

FIGURE 2 The experimental geometry (*left*). The *x-y* is the sample plane, and *z*-axis, the director, is perpendicular to the sample plane. (*A*) Light pulse, polarization along $\vec{e}_i$, impinges on the sample under an angle θ and the emission, polarization $\vec{e}_f$, is observed under an angle ϕ. These angles are defined with respect to the director of the sample, *z*. (*B*) The Euler angles. The Euler angles $(\varphi_i, \theta_i, 0)$ of the polarization direction $\vec{e}_i$ of the incident beam.

Basic relation of fluorescence depolarization

Fluorescence from a molecule is a two-photon process; first a photon is absorbed and the molecule undergoes a transition to an excited electronic state. The molecule then relaxes in a short period of time (fs-ps) to the first excited state from where fluorescence will occur. The characteristic time duration of the fluorescence process is nanoseconds. We shall assume that the process of fluorescence depolarization involves pure dipole transitions. For this case the time dependent intensity $I_{if}(t)$ at time t after excitation with a δ-pulse is given by (Zannoni et al., 1983).

$$I_{if}(t) = \langle (\vec{e}_i \cdot \vec{\mu}_0)^2 (\vec{e}_f \cdot \vec{\nu}_t)^2 \rangle F(t) \qquad (1)$$

Here the subscripts i and f denote the initial and final state and $\vec{e}_i$ and $\vec{e}_f$ define the states of the polarizers used in the experimental geometry. $F(t)$ is the isotropic fluorescence decay function and it describes the probability that the probe is still excited at time t after the excitation at $t = 0$. $\vec{\mu}_0$ and $\vec{\nu}_t$ denote respectively the orientations of the absorption dipole $\vec{\mu}$ at time $t = 0$ and the emission dipole $\vec{\nu}$ at time t with respect to the laboratory frame. The quadratic terms in Eq. 1 originate from first order perturbation theory (Merzbacher, 1961). The brackets $\langle \ldots\ldots \rangle$ denote an ensemble average over all the probe motions up to time t. Eq. 1 is the basic relation in the theory of fluorescence depolarization from reorientational processes. The Wigner matrices (Rose, 1957) provide a powerful formalism for carrying out the orientational transformations implicit in Eq. 1. The dot products in Eq. 1 can be rewritten in Wigner functions ($D^L_{mn}[\Omega]$) (Rose, 1957), as

$$(\vec{e}_i \cdot \vec{\mu}_0)^2 = \{2P_2[\cos(\vec{e}_i \cdot \vec{\mu}_0)] + 1\}/3 = [2D^2_{00}(\vec{e}_i \cdot \vec{\mu}_0) + 1]/3 \qquad (2a)$$

$$(\vec{e}_f \cdot \vec{\nu}_t)^2 = \{2P_2[\cos(\vec{e}_f \cdot \vec{\nu}_t)] + 1\}/3 = [2D^2_{00}(\vec{e}_f \cdot \vec{\nu}_t) + 1]/3 \qquad (2b)$$

where $P_2(x) = (3x^2 - 1)/2$, the Legendre polynomial of rank 2. On inserting Eqs. 2 in Eq. 1 we obtain

$$I_{if}(t) = \langle 1 + 2D^2_{00}(\Omega_0) + 2D^2_{00}(\Omega_t) + 4D^2_{00}(\Omega_0)D^2_{00}(\Omega_t) \rangle F(t)/9. \qquad (3)$$

Here Ω_0 and Ω_t denote the Euler angles of the absorption and emission dipoles with respect to the polarization directions of the light beams. The Wigner formalism is used to carry out the orientational transformations which are necessary to separate the geometrical factors and the intrinsic molecular effects. This is done by the repeated use of the closure relation (Zannoni et al., 1983; Merzbacher, 1961; Rose, 1957) for Wigner functions. The transformation from the laboratory frame to the absorption dipole in the molecular frame requires four successive steps. These transformations from the laboratory frame to the absorption dipole moment in the molecular frame at $t = 0$ and the corresponding steps to the emission dipole moment at time t can now be easily separated from the orientation of the electric field vectors in the laboratory frame.

Orientational transformations

The transformation from the laboratory frame to the orientation of the transition dipole fixed in the molecular frame is carried out in four steps. For the absorption dipole we have (*a*) the transformation from the sample director to the axis of the water/lipid cylinder, denoted by $\Omega_{SC} = (\zeta_i, \pi/2, 0)$; (*b*) the transformation from the axis of the cylinder to the local director on this cylinder, denoted by $\Omega_{CD} = (-\epsilon_i, -\pi/2, 0)$; (*c*) the transformation from the local director to the molecular frame of the probe molecule, denoted by $\Omega_{DM}(0) = (\alpha_i, \beta_i, 0)$; and (*d*) the transformation from the molecular frame to the transition dipole of the molecule, denoted by $\Omega_{MT} = (\alpha_\mu, \beta_\mu, 0)$.

Furthermore the polarization direction of the incident electric field relative to the director (*z*-axis) of the sample is denoted by $\Omega_{LS} = (\varphi_i, \theta_i, 0)$. Similarly the transformations from the laboratory frame to the orientation of the emission dipole in the molecular frame are described by the four transformations $\Omega'_{SC} = (\zeta_f, \pi/2, 0)$, $\Omega'_{CD} = (-\epsilon_f, -\pi/2, 0)$, $\Omega'_{DM}(t) = (\alpha_f, \beta_f, 0)$, and $\Omega'_{MT} = (\alpha_\nu, \beta_\nu, 0)$. The polarization direction of the fluorescence relative to the *z*-axis is denoted by $\Omega'_{LS} = (\varphi_f, \theta_f, 0)$. As a

result, Eq. 3 is written as

$$I_{if}(t) = \sum_{mnpqsuvw} \cdot \langle 1 + 2D^{2*}_{m0}(\Omega_{LS})D^{2}_{mn}(\Omega_{SC})D^{2}_{np}(\Omega_{CD})D^{2}_{pq}[\Omega_{DM}(0)]D^{2}_{q0}(\Omega_{MT}) + 2D^{2}_{u}(\Omega'_{LS})D^{2*}_{su}(\Omega'_{SC})D^{2*}_{sv}(\Omega'_{CD})D^{2*}_{vw}[\Omega'_{DM}(t)]D^{2*}_{w0}(\Omega'_{MT}) + 4D^{2*}_{m0}(\Omega_{LS})D^{2}_{s0}(\Omega'_{LS})D^{2}_{mn}(\Omega_{SC})D^{2*}_{su}(\Omega'_{SC})D^{2}_{np}(\Omega_{CD})D^{2*}_{uv}(\Omega'_{CD}) \cdot D^{2}_{pq}(\Omega_{DM})D^{2*}_{vw}(\Omega'_{DM})D^{2}_{q0}(\Omega_{MT})D^{2*}_{w0}(\Omega'_{MT})\rangle F(t)/9 \quad (4)$$

Symmetry considerations

The average in Eq. 4 requires the evaluation of at least $5^8 = 390{,}625$ terms. Fortunately the symmetry properties of the hexagonal H_{II} phase and the use of cylindrically symmetric probe molecules will reduce this number drastically.

As the orientational transformations are independent, the averages of the products appearing in Eq. 4 are simply the products of the averages.

$$D^{2}_{00}(\Omega_0) = \sum_{mnpq} D^{2*}_{m0}(\Omega_{LS})\langle D^{2}_{mn}(\Omega_{SC})\rangle \cdot \langle D^{2}_{np}(\Omega_{CD})\rangle\langle D^{2}_{pq}[\Omega_{DM}(0)]\rangle D^{2}_{q0}(\Omega_{MT}) \quad (5a)$$

$$D^{2}_{00}(\Omega_t) = \sum_{suvw} D^{2}_{s0}(\Omega'_{LS})\langle D^{2*}_{su}(\Omega'_{SC})\rangle \cdot \langle D^{2*}_{uv}(\Omega'_{CD})\rangle\langle D^{2*}_{vw}[\Omega'_{DM}(t)]\rangle D^{2*}_{w0}(\Omega'_{MT}). \quad (5b)$$

The uniaxial symmetry in the sample, cylinder, and the director frames is now used to simplify Eqs. 5 further because for each phase (Zannoni et al., 1983; Luckhurst et al., 1974; Nordio and Segre, 1979),

$$\langle D^{2}_{mn}(\Omega)\rangle = \langle D^{2}_{0n}(\Omega)\rangle\delta_{m0}. \quad (6)$$

Thus we obtain

$$\langle D^{2}_{00}(\Omega_{SC})\rangle\langle D^{2}_{00}(\Omega_{CD})\rangle\langle D^{2}_{0q}[\Omega_{DM}(0)]\rangle\delta_{m0}\delta_{n0}\delta_{p0} \quad (7a)$$

$$\langle D^{2*}_{00}(\Omega'_{SC})\rangle\langle D^{2*}_{00}(\Omega'_{CD})\rangle\langle D^{2*}_{0w}[\Omega'_{DM}(t)]\rangle\delta_{s0}\delta_{u0}\delta_{v0} \quad (7b)$$

and Eqs. 5 reduce to

$$\langle D^{2}_{00}(\Omega^0)\rangle = \frac{1}{4}D^{2}_{00}(\Omega_{LS})\sum_{q}\langle D^{2}_{0q}\rangle D^{2}_{0q}(\Omega_{MT}) = \frac{1}{4}D^{2}_{00}(\Omega_{LS})S_{\mu} \quad (8a)$$

$$\langle D^{2}_{00}(\Omega_t)\rangle = \frac{1}{4}D^{2}_{00}(\Omega'_{LS})\sum_{w}\langle D^{2}_{0w}\rangle D^{2}_{0w}(\Omega'_{MT}) = \frac{1}{4}D^{2}_{00}(\Omega'_{LS})S_{\nu}. \quad (8b)$$

The evaluation of the averages of the correlation product appearing in Eq. 4 is more elaborate. A rearrangement of the factors in this product leads to five independent terms:

$$\langle D^{2}_{00}(\Omega_0)\,D^{2}_{00}(\Omega_t)\rangle = \sum_{mnpqsuvw} D^{2*}_{m0}(\Omega_{LS})\,D^{2}_{s0}(\Omega'_{LS}) \langle D^{2}_{mn}(\Omega_{SC})\,D^{2*}_{su}(\Omega'_{SC})\rangle \langle D^{2}_{np}(\Omega_{CD})\,D^{2*}_{uv}(\Omega'_{CD})\rangle \langle D^{2}_{pq}[\Omega_{DM}(0)]\,D^{2*}_{vw}[\Omega'_{DM}(t)]\rangle \langle D^{2}_{q0}(\Omega_{MT})\,D^{2*}_{w0}(\Omega'_{MT})\rangle \quad (9)$$

Each of these factors will not be considered in detail: (*a*) The first contains the Euler angles $(\varphi_i, \theta_i, 0)$ and $(\varphi_F, \theta_f, 0)$ describing the experimental geometry as depicted in Fig. 2. (*b*) The second factor reduces the

$$\langle D^{2}_{mn}(\zeta_i, \pi/2, 0)\,D^{2*}_{mu}(\zeta_f, \pi/2, 0)\rangle\delta_{ns}, \quad (10)$$

because the axis of the water cylinder does not reorient on the time scale of the fluorescence process. (*c*) The third describes the time correlation between the orientation of the local director of the water cylinder at $t = 0$ and $t = t$. The local director can only undergo lateral diffusion on the surface of the water cylinder. On utilizing the uniaxial symmetry of the cylinder and using the explicit Euler angles we find

$$\langle D^{2}_{np}(\Omega_{CD})\,D^{2*}_{uv}(\Omega'_{CD})\rangle = D^{2}_{np}(0, -\pi/2, 0)\,D^{2*}_{uv}(0, -\pi/2, 0)\,\langle \exp[i(n\epsilon_i - u\epsilon_f)]\rangle. \quad (11)$$

The lateral displacement on the cylinder surface can be described as a diffusion process for which we have (Reichl, 1980)

$$\langle \exp[i(n\epsilon_i - u\epsilon_f)]\rangle = \exp(-n^2 D_{lat}t)\delta_{nu}. \quad (12)$$

Here the lateral diffusion of the probe on the cylinder surface is described by a single parameter, $D_{lat.}$ (*d*) The fourth factor describes the orientational correlation function with respect to the local director. It correlates the orientation between the long axis of the probe molecule at $t = 0$ and $t = t$. For the cylindrically symmetric probe molecules used here and on taking the local phase to be uniaxial, we have (Luckhurst et al. 1974; Nordio and Segre, 1979)

$$\langle D^{2}_{pq}[\Omega_{DM}(0)]\,D^{2*}_{vw}[\Omega'_{DM}(t)]\rangle = \langle D^{2}_{pq}[\Omega_{DM}(0)]\,D^{2*}_{pq}[\Omega'_{DM}(t)]\rangle\delta_{pv}\delta_{qw}. \quad (13)$$

(*e*) The last factor contains all the information about the orientations of the transition dipoles in the molecular frame and cannot be reduced any further. For the sake of brevity we shall henceforth use the following notation:

$$H_p = H_p(t) = \sum_{q}\langle D^{2}_{pq}[\Omega_{DM}(0)]D^{2*}_{pq}[\Omega'_{DM}(t)]\rangle \cdot D^{2}_{q0}(\alpha_\mu, \beta_\mu, 0)\,D^{2*}_{q0}(\alpha_\nu, \beta_\nu, 0)\delta_{pv}\delta_{qw}. \quad (14)$$

For cylindrically symmetric probe molecules $H_p(t) =$

$H_{-p}(t)$, p = 0, 1, 2 (Zannoni et al., 1983; Luckhurst et al., 1974; Nordio and Segre, 1979). The average of the product is now written as

$$\langle D^2_{00}(\Omega_0)\, D^2_{00}(\Omega_t)\rangle = \sum_{mnpvw} D^{2*}_{m0}(\varphi_i, \theta_i, 0)\, D^2_{m0}(\varphi_f, \theta_f, 0) \cdot D^2_{mn}(0, \pi/2, 0)\, D^{2*}_{mn}(0, \pi/2, 0) D^2_{np}(0, -\pi/2, 0) \cdot D^{2*}_{np}(0, -\pi/2, 0) \exp(-D_{lat} n^2 t)\, H_p. \quad (15)$$

On carrying out the summations and using the explicit expressions for the Wigner rotation matrix elements with the notation $\varphi_{if} = \varphi_i - \varphi_f$, we finally obtain

$$\begin{aligned} I_{if}(t) = F(t)\{&1/9 + P_2(\cos\theta_i)\, S_\mu + P_2(\cos\theta_f)\, S_\nu \\ &+ P_2(\cos\theta_i) P_2(\cos\theta_f)[2(H_0 + 3H_2) \\ &+ 3(3H_0 + 4H_1 + H_2)\exp(-4D_{lat}t)]/72 \\ &+ \sin(2\theta_i)\sin(2\theta_f)\cos(\varphi_{if})[4(H_1 + H_2)\exp(-D_{lat}t) \\ &+ (3H_0 + 4H_1 + H_2)\exp(-4D_{lat}t)]/48 \\ &+ \sin^2(\theta_i)\sin^2(\theta_f)\cos(2\varphi_{if})[6(H_0 + 3H_2) \\ &+ 16(H_1 + H_2)\exp(-D_{lat}t) \\ &+ (3H_0 + 4H_1 + H_2)\exp(-4D_{lat}t)]/192\} \end{aligned} \quad (16)$$

It is important to realize that in Eq. 16 the geometrical factors (θ_i, θ_f, φ_{if}) and the molecular properties [$F(t)$, S_μ, S_ν, H_0, H_1, H_2, D_{lat}] are completely separated.

Determination of the fluorescence decay

The fluorescence decay function $F(t)$ can be determined in a time-resolved experiment. An experimental geometry has to be found for which every contribution of the correlation functions $H_p(t)$, p = 0, 1, 2 to the time-dependent intensity defined in Eq. 16 disappears. It can be shown that this condition is fulfilled on setting θ_i = 36.3°, θ_f = 90°, φ_i = 90°, and φ_f = 45°. However, in practice these angles need to be corrected for refraction effects at the sample interface. For a lipid with a refractive index of 1.50 the following experimental geometry is used. Excite with light polarized horizontally under an angle θ = 60° and detect the fluorescence light along the normal to the sample surface (the director). The analyzer must be set at 45° with respect to the horiziontal plane. The observed signal is now proportional to $F(t)$.

Steady-state experiments

In angle-resolved steady-state experiments, the samples are illuminated continuously with linear polarized light. Therefore, instead of time-dependent intensities, their time integrals are measured. The following quantities are defined

$$A_\mu = \int_0^\infty [F(t)S_\mu/18]\,dt = S_\mu/18 \quad (17a)$$

$$A_\nu = \int_0^\infty [F(t)S_\nu/18]\,dt = S_\nu/18 \quad (17b)$$

$$A_0 = \int_0^\infty \{F(t)\,[2(H_0 + 3H_2) + 3(3H_0 + 4H_1 + H_2) \cdot \exp(-4D_{lat}t)]/72\}\,dt \quad (17c)$$

$$A_1 = \int_0^\infty \{F(t)\,[4(H_1 + H_2)\exp(-D_{lat}t) + (3H_0 + 4H_1 + H_2)\exp(-4D_{lat}t)]/48\}\,dt \quad (17d)$$

$$A_2 = \int_0^\infty \{F(t)\,[6(H_0 + 3H_2) + 16(H_1 + H_2)\exp(-D_{lat}t) + (3H_0 + 4H_1 + H_2)\exp(-4D_{lat}t)]/192\}\,dt. \quad (17e)$$

A propagating light wave in an uniaxial medium has two independent directions of the electric field. The first, the ordinary (o) ray, has its electric field polarized perpendicular to the plane of incidence and hence to the axis of symmetry for all angles of incidence. Under our experimental conditions the light is x-axis polarized so that $\theta_i = \theta_f = \pi/2$ and $\varphi_i = \varphi_f = 0$ (Fig. 2). The second, the extraordinary (e) ray, is polarized in the plane of incidence, in our case the horizontal zy-plane, and is defined by the angles $\theta_i = \pi/2 - \theta$, $\theta_f = \pi/2 - \varphi$, $\varphi_i = \pi/2$, and $\varphi_f = \pi/2$ (Fig. 2). We can now make use of four combinations of the polarization directions of the excitation and emission beams: oo, oe, eo, ee. The corresponding fluorescence intensities are: I_{oo}, I_{oe}, I_{eo}, and I_{ee}, where the subscripts denote the polarization of the incident and fluorescence light ray, respectively. Eq. 16 thus yields for the fluorescence intensities

$$I_{oo} = 1/9 - A_\mu/2 - A_\nu/2 + A_0/4 + A_2 \quad (18a)$$

$$I_{oe} = 1/9 - A_\mu/2 - (1 - 3\sin^2\varphi)A_\nu/2 + (1 - 3\sin^2\varphi)A_0/4 - (1 - \sin^2\varphi)A_2 \quad (18b)$$

$$I_{eo} = 1/9 - (1 - 3\sin^2\theta)A_\mu/2 - A_\nu/2 + (1 - 3\sin^2\theta)A_0/4 - (1 - \sin^2\theta)A_2 \quad (18c)$$

$$I_{ee} = 1/9 - (1 - 3\sin^2\theta)A_\mu/2 - (1 - 3\sin^2\varphi)A_\nu/2 + (1 - 3\sin^2\theta)(1 - 3\sin^2\varphi)A_0/4 - \sin(2\theta) \cdot \sin(2\varphi)A_1 + (1 - \sin^2\theta)(1 - \sin^2\varphi)A_2. \quad (18d)$$

To remove the dependence of unknown experimental quantities as the illuminated volume and the intensity of the exciting light, polarization ratios are determined. In angle-resolved experiments the polarization ratios $R_o = I_{oe}/I_{oo}$ and $R_e = I_{eo}/I_{ee}$ are observed as a function of the angles θ and φ. We find for the angle-dependent polarization ratios R_o and R_e for the ordinary and the extraordinary experiment, respectively.

$$R_o(\theta, \varphi) = [1 - R_1 + (R_1 + R_2)\sin^2(\varphi)]/[1 + R_1] \quad (19)$$

$$R_e(\theta, \phi) = [1 - R_1 + (R_1 + R_3)\sin^2(\theta)] / [1 + R_1 + (R_2 - R_1)\sin^2(\varphi) + (R_3 - R_1)\sin^2(\theta) + R_4 \sin(2\theta)\sin(2\varphi) + R_5 \sin^2(\theta)\sin^2(\varphi)] \quad (20)$$

Here the relations between the parameters R_1–R_5 describing the angle dependence of the observed polarization ratios and the five quantities describing the time integrated intensities are

$$R_1 = 9A_2/N \quad (21a)$$

$$R_2 = (27A_\nu/2 - 27A_0/4)/N \quad (21b)$$

$$R_3 = (27A_\mu/2 - 27A_0/4)/N \quad (21c)$$

$$R_4 = 9A_1/N \quad (21d)$$

$$R_5 = (81A_0/4 + 9A_2)/N \quad (21e)$$

with

$$N = 1 - 9(A_\mu + A_\nu)/2 + 9A_0/4. \quad (21f)$$

It should be noted here that Eqs. 19 and 20 are analogous to those derived for the description of angle-dependent fluorescence depolarization measurements on macroscopically ordered planar multibilayer systems (van Langen et al., 1987*a*; Deinum et al., 1988; Mulders et al., 1986; van der Meer et al., 1982; van Langen et al., 1988*a*). However the physical significance of the parameters R_1–R_5 is different than the ones given in Eqs. 21.

INTERPRETATION

Hexagonal phase

The quantities A_μ, A_ν, A_0, A_1, and A_2 contain all the information about the molecular behavior in the system. For the probe molecule TMA-DPH the absorption dipole coincides with the long axis of the probe molecule while the emission dipole is tilted away by an angle $\beta_{\mu\nu}$ (van Langen et al., 1987*a* and *b*, 1988*a* and *b*; Deinum et al., 1988; Mulders et al., 1986; Johansson and Lindblom, 1986; van Langen et al., 1989). On using Eq. 8, A_μ and A_ν can be simplified to

$$A_\mu = \langle P_2 \rangle/18 \quad (22a)$$

$$A_\nu = \langle P_2 \rangle P_2(\cos\beta_{\mu\nu})/18. \quad (22b)$$

We shall now show that the dynamic parameters as well as the order parameter $\langle P_4 \rangle = 1/8\langle 35\cos^4\beta - 30\cos^2\beta + 3\rangle$, where β denotes the angle between the long axis of the probe molecule and the local director, are contained in A_0, A_1, A_2. The orientational correlation functions $H_0(t)$, $H_1(t)$, and $H_2(t)$ for the proble molecules considered here are given by

$$H_p(t) = \langle D^2_{p0}(\Omega_{DM})\, D^{2*}_{p0}(\Omega'_{DM})\rangle\, P_2(\cos\beta_{\mu\nu}) = G_p(t)\, P_2(\cos\beta_{\mu\nu}), \quad p = 0, 1, 2 \quad (23)$$

The functions $G_p(t)$ correlate the orientation of the long axis at the time of absorption and at the time of emission. Because we have assumed a stochastic motional behavior, these molecular orientations are completely correlated at $t = 0$, but this correlation is totally lost at $t = \infty$. It can be shown that the limiting values of the correlation functions at $t = 0$ and $t = \infty$ can be obtained in terms of the order parameters $\langle P_2 \rangle$ and $\langle P_4 \rangle$ in a model independent way (Zannoni et al., 1983; Fisz, 1985; Fisz, 1987).

$$G_0(0) = 1/5 + 2\langle P_2\rangle/7 + 18\langle P_4\rangle/35 \quad (24a)$$

$$G_1(0) = 1/5 + \langle P_2\rangle/7 - 12\langle P_4\rangle/35 \quad (24b)$$

$$G_2(0) = 1/5 - 2\langle P_2\rangle/7 + 3\langle P_4\rangle/35 \quad (24c)$$

$$G_0(\infty) = \langle P_2\rangle^2 \quad (24d)$$

$$G_1(\infty) = G_2(\infty) = 0. \quad (24e)$$

The time decay of these functions, however, must be evaluated in terms of a motional model. We shall here use the rotational diffusion model (Luckhurst et al., 1974; Nordio and Segre, 1979) in which the probe molecules are assumed to undergo small step orientational diffusion subject to an angle-dependent ordering potential $U(\beta)$ which is taken to be of the form

$$U(\beta) = \lambda_2 P_2(\cos\beta) + \lambda_4 P_4(\cos\beta). \quad (25)$$

The rotational diffusion in this potential is described by the diffusion constants perpendicular and parallel to the long axis, $D_\perp$ and $D_{//}$, respectively. Because the absorption dipole coincides with the long axis of the probe molecule the experiments are only sensitive to the diffusion constant $D_\perp$. The decay of $G_p(t)$ is obtained from a numerical solution of the diffusion equation (Nordio and Segre, 1979) and it has been shown that $G_p(t)$ can be expressed as an infinite sum of exponentials.

$$G_p(t) = \sum_m b_{pm} \exp(-a_{pm} D_\perp t), \quad p = 0, 1, 2. \quad (26)$$

The preexponential factors b_{pm} and the decay coefficients a_{pm} are complex functions of the parameters λ_2 and λ_4. It is interesting to note that in most practical cases the slowest decay term dominates the decay of $G_p(t)$ (Nordio and Segre, 1979). Consequently this monoexponential form of $G_p(t)$ was used in our numerical calculations.

The fluorescence decay function of TMA-DPH molecules embedded in lipid systems is often found to be biexponential. It is now important to note that the intensi-

ties observed in steady-state experiments are determined by the time integrals of the decay terms, Eqs. 17. It is easy to show that in the time integral of the multiexponential decay, each decay component is weighted by its decay time. Consequently the slowest decay components make a large contribution to the integral and in our case it is in fact dominated by them. Thus, the steady-state experiment is much more sensitive to the decay component of the intrinsic fluorescence with the longest lifetime. We have previously shown in multibilayer systems that taking the fluorescence decay of TMA-DPH molecules to be monoexponential with the average fluorescence lifetime (τ_F) as decay time, introduces only small changes in the physical parameters (Deinum et al., 1988; Mulders et al., 1986; van Ginkel et al., 1986). Therefore we assume that the intrinsic decay function $F(t)$ has the simple form

$$F(t) = (1/\langle\tau_F\rangle) \exp(-t/\langle\tau_F\rangle) \quad (27)$$

By following this approach the time integrals appearing in the expressions for A_0, A_1, and A_2 are readily performed.

It is important to note that both the diffusion constant $D_\perp$ for the reorientational dynamics and D_{lat} for the lateral diffusion of the probe molecule on the water cylinder can be obtained. These will be expressed as the products $D_\perp\langle\tau_F\rangle$ and $D_{lat}\langle\tau_F\rangle$.

The orientational ordering is described by the orientational distribution function $f(\beta)$. This function describes the probability of finding a probe oriented with an angle β with respect to the local director of the system. It is shown that this function takes the form (van Ginkel et al., 1986; van Gurp et al., 1988)

$$f(\beta) = N_0 \exp[-U(\beta)], \quad (28)$$

where N_0 is a normalization constant. From this distribution function the order parameters $\langle P_2\rangle$ and $\langle P_4\rangle$ are calculated. The number density of probe molecules oriented at β is given by $f(\beta)$ sin (β) and is normalized to unity.

The model parameters describing the angle-resolved depolarization measurements are λ_2, λ_4, $D_\perp\langle\tau_F\rangle$, $D_{lat}\langle\tau_F\rangle$ and $\beta_{\mu\nu}$. These five model parameters are contained in the experimentally observed values for R_1–R_5.

Oriented planar multibilayers

In planar multibilayers the orientational order is characterized by the order parameters $\langle P_2\rangle$ and $\langle P_4\rangle$. Now β is the angle between the macroscopic director, the normal to the bilayer surface, and the long axis of the probe molecule. Furthermore only the diffusion constant $D_\perp$ determines the decay of the correlation functions Eq. 26, as the experiments are not sensitive to lateral diffusion of the probe molecule over the bilayer plane. Here only four parameters, λ_2, λ_4, $D_\perp\langle\tau_F\rangle$ and $\beta_{\mu\nu}$ are contained in R_1–R_5 (van Langen et al., 1987*a*; Deinum et al., 1988; Mulders et al., 1986; van der Meer et al., 1982; van Ginkel et al., 1986).

Evaluation of the model parameters

Values for the model parameters were obtained from a direct nonlinear least squares fit of the measured depolarization ratios at 56 different combinations of the angles θ and φ, to Eq. 20. The five parameters R_1–R_5 appearing in Eq. 20 were evaluated in terms of the model parameters using Eqs. 17 and 21–27. The ZXSSQ routine of the IMSL library was used in the search for the minimum in χ^2. The errors were determined from the Hessian matrix produced by the ZXSSQ routine. No significant correlations between the model parameters were found. This procedure has been described by us previously (Deinum et al., 1988; van Gurp et al., 1988; van Langen et al., 1987*a*; Mulders et al., 1986) and shown to be reliable and numerically stable. We note that the parameters R_1–R_5 can also be determined with this procedure.

MATERIALS AND METHODS

Sample preparations

The lipid DOPE was the kind gift of Prof. B. de Kruijff (Institute of Molecular Biology, University of Utrecht) and used without further purification. The fluorescent probe TMA-DPH was purchased from Molecular Probes Inc., Eugene, OR, and used as received. The probe was dissolved in absolute ethanol and stored under nitrogen atmosphere in the dark at 4°C. Macroscopically ordered lipid systems between thin (175 μm) microscope coverglasses were prepared as follows. 10 mg of lipids were dissolved in a chloroform ethanol solution and the probe solution, 5.10^{-4} M, was added to obtain a probe-to-lipid ratio of 1:250 on a molecular basis. The solvents were evaporated by a flow of nitrogen, and the dried lipid probe mixture was kept overnight under vacuum. The lipids were equilibrated for 48 h at 5°C in a humidified (96% relative humidity) nitrogen atmosphere over a saturated K_2SO_4 salt solution in an exiccator. The samples were prepared in the lamellar phase at 5°C. 2 mg of the hydrated mixture was placed on a microscope glass plate 24 × 24 mm, using a spatula. A second plate, 20 × 20 mm, was pressed on the mixture and a macroscopically aligned multibilayer system was obtained by gently rubbing the two glass slides against each other. The edges of this sandwich were sealed with a two-component epoxy resin and the quality of alignment was checked with a polarizing microscope equipped with a first order red plate. Only homogeneously colored samples were used further. A round spot, diameter 4 mm, was masked off with black tape and used in the experiments. During the preparative steps the samples were kept as much as possible in dark at 5°C.

Steady-state experiments

A home-built fluorimeter was used to perform the angle-resolved fluorescence depolarization experiments. Excitation light, wavelength 360 ± 5 nm, is selected by a monochromator (Bausch and Lomb,

Rochester, NY) from a 450 W Xenon arc lamp. This beam is polarized by a Glan-Thompson prism in the horizontal zy-plane (Fig. 2) before incidence on a rotatable, temperature-controlled sample holder. A sheet polarizer and filter combination (a GG 395 cut off filter and a 447 ± 13 nm interference filter, both from Schott, Mainz, FRG) define the wavelength of the fluorescence light. A Peltier cooled photomultiplier (RCA-31034, Lancaster, PA) is used to detect the fluorescence light. The light intensity is defined by the number of photons counted in a preset period of time. An Apple II microcomputer (Cupertino, CA) is used for the data acquisition. In the extraordinary experiments performed here the intensity ratio, $I_{ee}/I_{eo} = 1/R_e$, is determined for 56 different combinations of θ and φ. Control experiments with blank samples have shown that the background intensity is <1% of the fluorescence signal. The experimental error in the observed ratio is in the order of 2%.

For a sample in the lamellar L_α phase, the temperature was kept at 7°C and for the same sample in the hexagonal H_{II} phase the temperature was 45°C. No coexistence of the phases is expected at these temperatures (Cullis and de Kruijff, 1978; Cullis et al., 1980). The refractive index of the samples was measured with an Abbe-refractometer and values between 1.48 and 1.50 were found. The angles in the sample are determined by using Snell's law on taking the refractive index of the sample equal to 1.5. A slight birefringence of ~0.02 is observed. Optical corrections due to birefringence are smaller than the experimental error and were neglected. It has been shown theoretically (van Ginkel et al., 1986; van Gurp et al., 1988) that there is no need to correct for the effects of multiple reflections within the sample and transmission losses at the sample/air interfaces. This was verified experimentally with refractive index matching methods. The sample was mounted in a cuvette filled with a clear liquid with the same refractive index. The geometry of the cuvette constrains the exciting and emitting light beams to be perpendicular. The experimental polarization ratios were found to be the same as those obtained from corresponding angles with the sample in air. These latter experiments suffer from the disadvantage that the angles θ and φ cannot be varied independently.

RESULTS AND DISCUSSION

Macroscopically aligned samples of lipid systems either in the lamellar L_α or in the hexagonal H_{II} phase appear to be optically homogeneous under the polarizing microscope and thus are particularly amenable for studies with fluorescence depolarization techniques. We have shown previously how angle-resolved fluorescence depolarization techniques can be used with aligned samples for the determination of the molecular orientational order and dynamics of the fluorescent probe molecules (van Langen et al., 1987*a*; Deinum et al., 1988; Mulders et al., 1986). In these experiments the sample is excited with light polarized in the horizontal zy-plane (Fig. 2), the extraordinary experiment, and the angle-dependence of the polarization ratios, $I_{ee}/I_{eo} = 1/R_e$, is measured.

The observed fluorescence intensity was found to be considerably higher in the hexagonal phase than in the lamellar phase. This is due to the fact that the probe molecules in the lamellar phase are preferentially oriented with their long axis perpendicular to the sample plane and are therefore not excited efficiently by the incident beam.

The polarization ratios $1/R_e$ at 56 different combinations of the angles θ and ϕ were measured in the extraordinary experiment where the incident excitation light is horizontally polarized. The angle dependence of the polarization ratios obtained from these two phases is clearly seen to be markedly different (Fig. 3). This is also reflected in the values of R_1–R_5, presented in Table 1. These parameters were extracted by fitting the experimental ratios to Eq. 20 with a nonlinear least squares procedure (Deinum et al., 1988; van Gurp et al., 1988; van Langen et al., 1987*a*; Mulders et al., 1986). The best theoretical fit to the observations from the lamellar and hexagonal phase of DOPE are also shown in Fig. 3. Numerical simulations of the polarization ratios have, however, shown that the R_1–R_5 values for the hexagonal phase are much more sensitive to random errors than those for the lamellar one.

To interpret the experimental results in terms of the physical parameters describing the orientational order and dynamics, the rotational diffusion model is used. In general, this model requires the determination of two diffusion constants and an angle-dependent potential. We note that the correlation functions $G_p(t)$ describing the rotational dynamics (Eq. 26) are now obtained from a

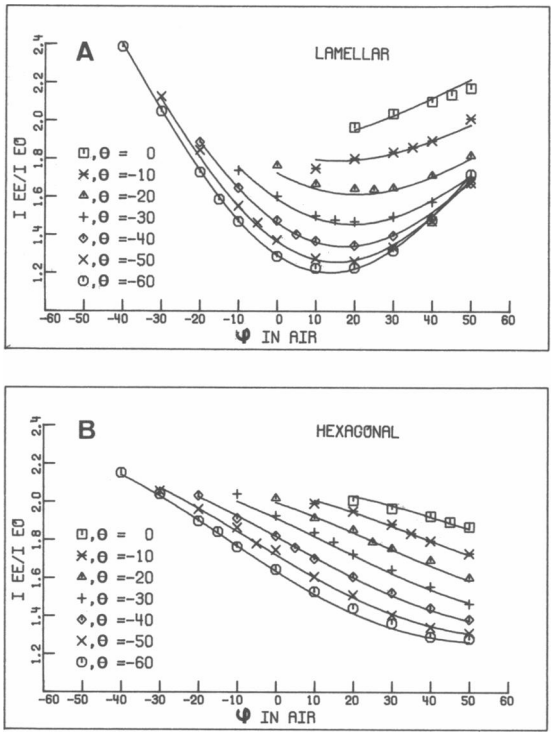

FIGURE 3 The angle φ dependence of 56 experimentally observed polarization ratios $1/R_e$ for different angles of incidence θ together with their best fit. (*A*) The lamellar L_α phase at 7°C and (*B*) the hexagonal H_{II} phase at 45°C of TMA-DPH in DOPE.

TABLE 1 Summary of recovered values for the parameters R_1–R_5

	Lamellar L_α phase	Hexagonal H_{II} phase
Temperature (°C)	7	45
No. of experiments	3	2
R_1	0.34 (0.02)	0.36 (0.02)
R_2	1.1 (0.10)	−0.22 (0.05)
R_3	1.7 (0.10)	−0.11 (0.03)
R_4	0.95 (0.10)	0.44 (0.02)
R_5	13.0 (1.5)	2.60 (0.20)

Errors are given in parentheses.

numerical solution of the diffusion equation. The potential $U(\beta)$, given in Eq. 25, has been used in the analysis of the experimental data of both phases. This potential has been chosen as the pair of coefficients (λ_2, λ_4) yields unique values for the order parameters $\langle P_2 \rangle$ and $\langle P_4 \rangle$ (Mulders et al., 1986; van Ginkel et al., 1986; van Gurp et al., 1988). Its validity, however, is open to question as we do not expect the probe molecule TMA-DPH to be oriented in the hexagonal phase at angles $\beta > 90°$ or $\beta < -90°$ relative to the local director. This, because the molecules are anchored with their polar headgroup at the aqueous interface (Prendergast et al., 1981). Nevertheless, we have shown previously in the case of vesicle systems, where the same arguments apply, that the simplest potential satisfying this restriction, $U(\beta) = \lambda_1 \cos(\beta) + \lambda_2 P_2[\cos(\beta)]$, fails to describe the experiments (van Langen et al., 1988*b*). Unfortunately a more extended and realistic potential cannot be used as it requires more parameters in its description than can be determined with this technique.

The behavior of the molecules in the lamellar phase is described by four model parameters λ_2, λ_4, $D_\perp\langle\tau_F\rangle$, $\beta_{\mu\nu}$, whereas five parameters λ_2, λ_4, $D_\perp\langle\tau_F\rangle$, $D_{lat}\langle\tau_F\rangle$, $\beta_{\mu\nu}$ are required for the description of the behavior in the hexagonal phase. The extracted values obtained from a direct fit to the experimental data as described above, are shown in Table 2 together with corresponding order parameters $\langle P_2 \rangle$ and $\langle P_4 \rangle$. The orientational distribution function $f(\beta)$ and the number density function $f(\beta)\sin(\beta)$ for both phases, are shown in Fig. 4. The probe molecules are found to be oriented preferentially along the normal to the lipid/water interface. Whereas the function for the lamellar phase shows a monotonic decrease towards $\beta = \pm 90°$, a somewhat bimodal orientational distribution is found in the hexagonal phase. Nevertheless in the hexagonal phase the distribution around $\beta = 0°$ is considerably narrower than that of the lamellar phase. The population of probes oriented at $\beta = 90°$ may be an artefact due to the assumptions used in the analysis. We have here approximated a small surface element of the curved cylinder by a planar surface. Nevertheless, they may well be the result of the edge effects of finite cylinders or effects of cylinders which are not perfectly aligned parallel to the glass plates of the sample. It is interesting to note in this connection that we have observed bimodal distributions for TMA-DPH molecules in highly curved small unilamellar lipid vesicles (van Langen et al., 1989).

TABLE 2 Model parameters and order parameters

	Lamellar L_α phase	Hexagonal H_{II} phase
λ_2	−2.4 (0.2)	−1.2 (0.2)
λ_4	−0.63 (0.1)	−3.9 (0.4)
$D_\perp\langle\tau_F\rangle$	0.08 (0.01)	0.11 (0.01)
$D_{lat}\langle\tau_F\rangle$	Not obtainable	0.01 (0.005)
$\beta_{\mu\nu}$	15° (2)	20° (2)
$\langle P_2 \rangle$	0.60 (0.01)	0.74 (0.02)
$\langle P_4 \rangle$	0.30 (0.02)	0.66 (0.03)

Errors are given in parentheses.

The results for the hexagonal phase reveal that the process of lateral diffusion over the cylindrical water tube is at least 10 times slower than the process of the reorientational motion. Experiments on vesicle systems with other techniques support this observation (Houslay and Stanley, 1982). We can now estimate the value of the diffusion coefficients for the reorientational motion on using the average fluorescent lifetime of 3.4 ± 0.2 ns obtained from a time-resolved experiment at 20°C (data

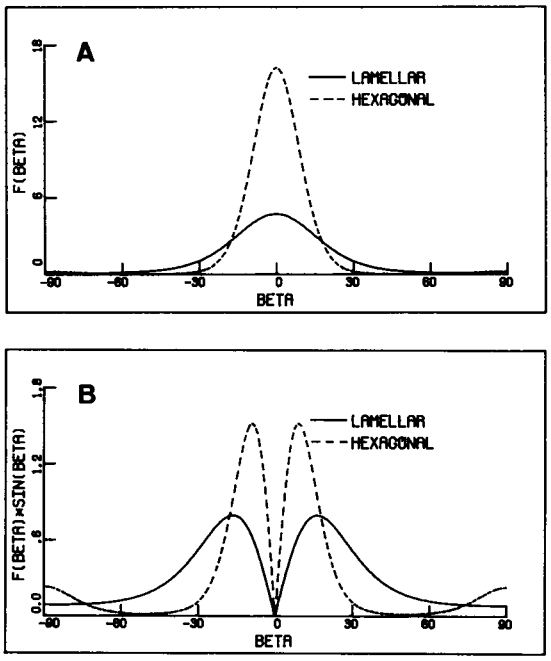

FIGURE 4 (*A*) The orientational distribution function $f(\beta)$. (*B*) The number density function $f(\beta)\sin(\beta)$ for TMA-DPH in the lamellar L_α phase at 7°C and the hexagonal H_{II} phase at 45°C.

not shown). On assuming that the average lifetime does not change drastically with temperature, we conclude that the diffusion coefficient $D_\perp$ in the hexagonal phase is comparable with that in the lamellar phase.

The experiments yielded significant values for the angle $\beta_{\mu\mu}$ between the transition dipoles of TMA-DPH. Similar values for the angle were also found in various other lipid vesicle systems (van Langen et al., 1987*b* and 1988*b*; van Langen et al., 1989) or planar multibilayer systems (Deinum et al., 1988; Mulders et al., 1986) and it was found to depend on environmental conditions (van Langen et al., 1987*a*).

The values of the order parameters and the diffusion constant obtained in the lamellar phase of DOPE are similar to those reported in multibilayer systems of various unsaturated phosphatidylcholine (PC) lipids (Deinum et al., 1988). In spite of the temperature differences in the experiments, the diffusion constants in DOPE and DOPC are the same, whereas the order parameters found in DOPE are somewhat higher as the ones reported for DOPC (Deinum et al., 1988).

We have here demonstrated the potential of steady-state fluorescence depolarization experiments in studies of lipid systems arranged in the hexagonal phase. Work is currently in progress to obtain more detailed information about molecular order and dynamics from angle- and time-resolved experiments on lipid systems in the hexagonal phase.

The investigations were made possible by the financial support given to Dr. van Langen by the Dutch Foundation for Biophysics under the auspices of the Netherlands Organization for Scientific Research.

Received for publication 27 September 1988 and in final form 30 November 1988.

REFERENCES

Bentz, J., H. Ellens, and F. C. Szoka. 1987. Destabilization of phosphatidylethanolamine-containing liposomes: hexagonal phase and asymmetric membranes. *Biochemistry.* 26:2105–2116.

Blaurock, A. E. 1982. Evidence of bilayer structure and of membrane interactions from x-ray diffraction analysis. *Biochim. Biophys. Acta.* 650:167–207.

Boggs, J. M., and J. C. Hsia. 1973. Orientation and motion of amphiphilic spin labels in hexagonal lipid phases. *Proc. Natl. Acad. Sci. USA.* 70:1406–1409.

Brown, P. M., J. Steers, S. W. Hui, P. L. Yeagle, and J. R. Silvius. 1986. Role of head group structure in the phase behaviour of amino phospholipids. 2. Lamellar and nonlamellar phases of unsaturated phosphatidylethanolamine analogues. *Biochemistry.* 25:4259–4267.

Büldt, G. , H. U. Gally, A. Seelig, J. Seelig, and G. Zaccai. 1978. Neutron diffraction studies on selectively deuterated phospholipid bilayers. *Nature (Lond.).* 271:182–184.

Caffrey, M. 1985. Kinetics and mechanism of the lamellar gel/lamellar liquid-crystal and lamellar/inverted hexagonal phase transition in phosphatidylethanolamine: a real-time x-ray diffraction study using synchrotron radiation. *Biochemistry.* 24:4826–4844.

Crowe, J. H., L. M. Crowe, J. F. Carpenter, A. S. Rudolph, C. A. Wistrom, B. J. Spargo, and T. J. Anchordoguy. 1988. Interactions of sugars with membranes. *Biochim. Biophys. Acta.* 947:367–384.

Cullis, P. R., and B. de Kruijff. 1978. The polymorphic phase behaviour of phosphatidylethanolamines of natural and synthetic origin. A ^{31}P NMR study. *Biochim. Biophys. Acta.* 513:31–42.

Cullis, P. R., B. de Kruijff, M. J. Hope, R. Nayar, and S. L. Schmid. 1980. Phospholipids and membrane transport. *Can. J. Biochem.* 58:1091–1100.

Deinum, G., H. van Langen, G. van Ginkel, and Y. K. Levine. 1988. Molecular order and dynamics in planar lipid bilayers: effects of unsaturation and sterols. *Biochemistry.* 27:852–860.

de Kruijff, B., P. R. Cullis, A. J. Verkleij, M. J. Hope, C. J. A. van Echteld, and T. F. Taraschi. 1985*a*. Lipid polymorphism and membrane function. *In* Enzymes of Biological Membranes. A. Martonosi, editor. Plenum Publishing Corp., New York. 131–204.

de Kruijff, B., P. R. Cullis, A. J. Verkleij, M. J. Hope, C. J. A. van Echteld, T. F. Taraschi, P. van Hoogevest, J. A. Killian, A. Rietveld, and A. T. M. van der Steen. 1985*b*. Modulation of lipid polymorphism by lipid-protein interactions. *In* Progress in Protein-Lipid Interactions. A. Watts and J. J. H. H. M. de Pont, editors. Elsevier Science, Amsterdam. 89–142.

Ellens, H., J. Bentz, and F. C. Szoka. 1986. Destabilization of phosphatidylethanolamine liposomes at the hexagonal phase transition temperature. *Biochemistry.* 25:285–294.

Fisz, J. J. 1985. Fluorescence depolarization in macroscopically ordered uniaxial molecular samples. *Chem. Phys.* 99:177–191.

Fisz, J. J. 1987. Symmetry simplifications in the description of molecular order and reorientational dynamics in uniaxial molecular systems. I. Symmetry constraints on the joint probability distribution function. *Chem. Phys.* 114:165–185.

Gasset, M., J. A. Killian, H. Tournois, and B. de Kruijff. 1988. Influence of cholesterol on gramicidin-induced H_{II} phase formation in phosphatidylcholine model membranes. *Biochim. Biophys. Acta.* 939:79–88.

Gruner, S. M. 1985. Intrinsic curvature hypothesis for biomembrane lipid composition: a role for nonbilayer lipids. *Proc. Natl. Acad. Sci. USA. 82:3665–3669.*

Hardman, P. D. 1982. Spin-label characterization of the lamellar-to-hexagonal (H_{II}) phase transition in egg phosphatidylethanolamine aqueous dispersions. *Eur. J. Biochem.* 124:95–101.

Hong, K., P. A. Baldwin, T. M. Allen, and D. Papahadjopoulos. 1988. Fluorometric detection of the bilayer-to-hexagonal phase transition in liposomes. *Biochemistry.* 27:3947–3955.

Houslay, M. D., and K. K. Stanley. 1982. Dynamics of Biological Membranes. John Wiley & Sons Ltd., Chichester, UK.

Israelachvili, J. N., and D. J. Mitchell. 1975. A model for the packing of lipids in bilayer membranes. *Biochim. Biophys. Acta.* 389:13–19.

Israelachvili, J. N., S. Marcelja, and R. G. Horn. 1980. Physical principles of membrane organization. *Q. Rev. Biophys.* 13:121–200.

Kirk, G. L., S. M. Gruner, and D. L. Stein. 1984. A thermodynamic model of the lamellar to inverse hexagonal phase transition of lipid membrane-water systems. *Biochemistry.* 23:1093–1102.

Lasić, D. D., and H. Hauser. 1984. Detection of hexagonal phases by ESR spin labeling. *Mol. Cryst. Liq. Cryst.* 113:59–75.

Luckhurst, G. R., M. Setaka, and C. Zannoni. 1974. An electron

resonance investigation of molecular motion in the smectic A mesophase of a liquid crystal. *Mol. Phys.* 28:49–68.

Luzzati, V., T. Gulik-Krzywicki, and A. Tardieu. 1968. Polymorphism of lecithins. *Nature (Lond.).* 218:1031–1034.

Marsh, D., and J. M. Seddon. 1982. Gel-to-inverted hexagonal (L_β-H_{II}) phase transitions in phosphatidylethanolamines and fatty acid-phosphatidylcholine mixtures, demonstrated by ^{31}P-NMR spectroscopy and x-ray diffraction. *Biochim. Biophys. Acta.* 690:117–123.

Mely, B., J. Charvolin, and P. Keller. 1975. Disorder of lipid chains as a function of their lateral packing in lyotropic liquid crystals. *Chem. Phys. Lipids.* 15:161–173.

Merzbacher, E. 1961. Quantum Mechanics. John Wiley & Sons, New York.

Mulders, F., H. van Langen, G. van Ginkel, and Y. K. Levine. 1986. The static and dynamic behaviour of fluorescent probe molecules in lipid bilayers. *Biochim. Biophys. Acta.* 859:209–218.

Nordio, P. L., and U. Segre. 1979. The Molecular Physics of Liquid Crystals. G. R. Luckhurst and G. W. Gray, editors. Academic Press, London. 411–426.

Prendergast, F. G., R. P. Haugland, and P. J. Callahan. 1981. 1-[4(Trimethylamino)phenyl]-6-phenylhexa-1,3,5-triene: synthesis, fluorescence properties, and use as a fluorescence probe of lipid bilayers. *Biochemistry.* 20:7333–7338.

Ranck, J. L., T. Keira, and V. Luzzati. 1977. A novel packing of the hydrocarbon chains in lipids. The low temperature phases of dipalmitoyl phosphatidyl-glycerol. *Biochim. Biophys. Acta.* 488:432–441.

Reichl, L. E. 1980. A Modern Course in Statistical Physics. University of Texas Press, Austin. 167.

Reiss-Husson, F. 1967. Structure des phases liquide-crystallines de différents phospholipides, monoglycérides, sphingolipides, anhydres ou en présence d'eau. *J. Mol. Biol.* 25:363–382.

Rilfors, L., G. Lindblom, Å. Wieslander, and A. Christiansson. 1984. Lipid bilayer stability in biological membranes. *In* Membrane Fluidity. Vol. 12. M. Kates and B. Manson, editors. Plenum Publishing Corp., New York. 205–245.

Rose, M. E. 1957. Elementary Theory of Angular Momentum. John Wiley & Sons, New York.

Siegel, D. P. 1986*a*. Inverted micellar intermediates and the transitions between lamellar, cubic, and inverted hexagonal lipid phases. I. Mechanism of the $L_\alpha \leftrightarrow H_{II}$ phase transitions. *Biophys. J.* 49:1155–1170.

Siegel, D. P. 1986*b*. Inverted micellar intermediates and the transitions between lamellar, cubic, and inverted hexagonal lipid phases. II. Implications for membrane-membrane interactions and membrane fusion. *Biophys. J.* 49:1171–1183.

Sjölund, M., G. Lindblom, L. Rilfors, and G. Arvidson. 1987. Hydrophobic molecules in lecithin-water systems. I. Formation of reversed hexagonal phases at high and low water contents. *Biophys. J.* 52:145–153.

Tate, M. W., and S. M. Gruner. 1987. Lipid polymorphism of mixtures of dioleoylphosphatidylethanolamine and saturated and monounsaturated phosphatidylcholines of various chain lengths. *Biochemistry.* 26:231–236.

van der Meer, B. W., R. P. H. Kooyman, and Y. K. Levine. 1982. A theory of fluorescence depolarization in macroscopically ordered membrane systems. *Chem. Phys.* 66:39–50.

van Ginkel, G., L. J. Korstanje, H. van Langen, and Y. K. Levine. 1986. The correlation between molecular orientational order and reorientational dynamics of probe molecules in lipid multibilayers. *Faraday Discuss. Chem. Soc.* 81:49–61.

van Gurp, M., H. van Langen, G. van Ginkel, and Y. K. Levine. 1988. Angle-resolved techniques in studies of organic molecules in ordered systems using polarized light. *In* Polarized Spectroscopy of Ordered Systems. B. Samori' and E. W. Thulstrup, editors. Kluwer Academic Publishers Group, Dordrecht, Netherlands. 455–489.

van Langen, H., D. Engelen, G. van Ginkel, and Y. K. Levine. 1987*a*. Headgroup hydration in egg-lecithin multibilayers affects the behaviour of DPH probes. *Chem. Phys. Lett.* 138:99–104.

van Langen, H., Y. K. Levine, M. Ameloot, and H. Pottel. 1987*b*. Ambiguities in the interpretation of time-resolved fluorescence anisotropy measurements on lipid vesicle systems. *Chem. Phys. Lett.* 140:394–400.

van Langen, H., G. van Ginkel, and Y. K. Levine. 1988*a*. Fluorescence depolarization studies of molecular dynamics using pulsed synchrotron radiation: applications to lipid vesicles and oriented multibilayers. *In* Time-Resolved Laser Spectroscopy in Biochemistry. J. R. Lakowicz, editor. Society of Photo-Optical Instrumentation Engineers, Bellingham, WA. 377–388.

van Langen, H., G. van Ginkel, and Y. K. Levine. 1988*b*. A comparison of the molecular dynamics of fluorescent probes in curved lipid vesicles and planar multibilayers. *Liquid Crystals.* 3:1301–1317.

van Langen, H., G. van Ginkel, D. Shaw, and Y. K. Levine. 1989. The fidelity of response by TMA-DPH in time-resolved fluorescence anisotropy measurements on lipid vesicles. *Eur. Biophys. J.* In press.

van Venetië, R., and A. J. Verkleij. 1981. Analysis of the hexagonal II phase and its relations to lipidic particles and the lamellar phase. A freeze-fracture study. *Biochim. Biophys. Acta.* 645:262–269.

Zannoni, C., A. Arcioni, and P. Cavatorta. 1983. Fluorescence depolarization in liquid crystals and membrane bilayers. *Chem. Phys. Lipids.* 32:179–250.